

AN INVESTIGATION OF CLOUD DISTRIBUTION FROM SATELLITE INFRARED RADIATION DATA

ROBERT C. LO and DONALD R. JOHNSON

Department of Meteorology, The University of Wisconsin, Madison Wis.

ABSTRACT

A physical-statistical model using Nimbus II MRIR (medium resolution infrared) radiometer channel 2 (10–11 μm) data is formed to estimate cloud cover. In the model, cloud cover is estimated from the probability density distribution of DV2 values defined to be the differences between the earth surface temperatures and the corresponding channel 2 observed equivalent black-body temperatures. For cloud type estimation, channel 1 (6.4–6.9 μm) and channel 2 (10–11 μm) data are used simultaneously in a joint distribution model. Bivariate DV1 and DV2 frequency distributions portray distinct features associated with different cloud patterns from which it was possible to estimate the cloud coverage for different levels in the troposphere. The major limiting factor in estimating cloud coverage in this study was the areal resolution of the MRIR radiometer. The results indicate that a reliable global climatology may be formed, using higher resolution radiometers combined with irradiance information from other spectral intervals.

1. INTRODUCTION

One of the major problems in atmospheric heat budget studies is the specification of the global cloud distribution and the release of latent heat. Not only is heat realized by the condensation through convection but the cloud distribution also strongly influences reflection and direct absorption of solar energy as well as the flux of infrared radiation. One major limitation of the energy budget studies conducted prior to the satellite era that was fully recognized by authors was the limited data available for oceanic areas (e.g., Houghton 1954 and London 1951).

As a result of the meteorological satellite, irradiance data and cloud pictures are now available for oceanic areas; and the opportunity exists for the development of a comprehensive global climatology of cloud distribution. For maximum utility, the global cloud climatology must include information concerning the vertical as well as the horizontal distribution of cloud cover and types. Such information would aid in the specification of the release of latent heat and the influence of clouds on radiative transfer (Manabe and Möller 1961, Davis 1963, and Katayama 1966). Rasool (1964), Arking (1964), Winston and Taylor (1967), and others have already initiated such studies. However, several problems concerning the inference of cloud distribution from irradiance information remain. Among the problems are areal and spectral resolution of the instrument, variable atmospheric emissivity,

and the reduction of the information to manageable and meaningful statistics.

The aim of this paper is to develop a model using satellite radiation data and statistical considerations to estimate the areal distribution of the cloud cover and to study techniques to infer cloud type and height. Channel 1 (6.4–6.9 μm) and channel 2 (10–11 μm) MRIR (medium resolution infrared) radiometer data from Nimbus II are used in the estimation model to form bivariate and marginal frequency distributions from which the cloud distributions are inferred.

2. CONCEPTS, TECHNIQUES, AND PROCEDURES

A significant portion of the infrared radiation emitted by the earth's surface is absorbed by the atmospheric constituents—water vapor, carbon dioxide, and ozone. The atmosphere is, however, nearly transparent to the flux of black-body radiation emitted by the earth's surface in the 8- to 12- μm region of the infrared spectrum. Because of this selective absorption, satellite observations of infrared radiation flux within different regions of the infrared spectrum can be indicative of the content and distribution of the absorbing constituents.

The intensity of absorption and re-emission within the atmosphere depends on the distribution of the selective absorbing constituents. In spectral regions of strong absorption, the infrared energy emitted by the earth's

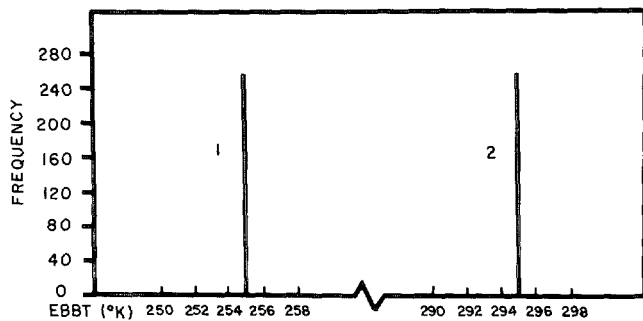


FIGURE 1.—Frequency histogram of equivalent black-body temperatures (EBBT) for an idealized model.

surface is almost completely absorbed and re-emitted at a lower temperature within the troposphere. Because the absorption and re-emission process may effectively occur many times, the stronger the absorption, the lower will be the characteristic temperature of re-emitted energy sensed by the satellite. In spectral regions of strong absorption, satellite observations are indicative of the distribution of absorbing constituents within the upper troposphere; and in regions of weak absorption, observations are indicative of the earth's surface temperature.

The MRIR radiometer on Nimbus II was designed with four channels to measure the infrared flux in different spectral regions, two of which are channel 1 (the water vapor band from 6.4–6.9 μm) and channel 2 (the window region from 10–11 μm). Because of the strong selective absorption by water vapor in the 6.4- to 6.9- μm region, channel 1 observations are indicative of the water vapor content of the upper portion of a clear atmosphere. In contrast, the channel 2 observations provide good estimates of the surface temperature, since a clear atmosphere is nearly transparent in the infrared region of the window channel. In an atmosphere with liquid and solid forms of water, the atmosphere tends to be uniformly opaque. Consequently, channel 2 data are either estimates of surface temperatures under clear skies or cloud-top temperatures under overcast conditions.

In the development of an idealized model for a partly cloudy region, we assume that (1) the clouds are of one type with a characteristic cloud-top temperature, (2) the atmosphere is perfectly transparent within the window region, (3) the satellite sensor has perfect resolution, (4) the tropospheric temperature decreases with height, (5) the surface temperature is constant, and (6) the clouds are effectively black with respect to the infrared flux. Under these assumptions, a histogram of channel 2 equivalent black-body temperature from a partially cloud-covered region would be described by two discrete lines. Figure 1 portrays a hypothetical sample composed of an equal number of observations from a cloudy region with a cloud-top temperature of 255°K and from a clear region with a surface temperature of 295°K.

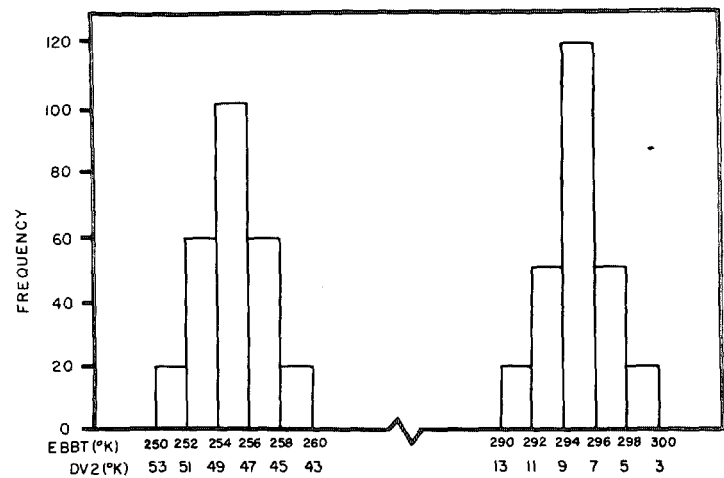


FIGURE 2.—Frequency histogram of equivalent black-body temperature for a realistic model.

Under the additional assumption that the observations are evenly distributed in the region of interest, the relative frequency of each peak becomes an estimate of the fractional area of either the cloudy or clear region. In figure 1, the fractional cloud cover is one-half.

In the atmosphere, cloud thickness and cloud-top height (and thus cloud-top temperature) vary. Also, the window region of the atmosphere is not perfectly transparent; and the outgoing irradiance is modified, however slightly, by the variable absorbing constituents. Thus, in the model's application to real situations, the channel 2 histogram will not be represented by two discrete lines. Some insight into its expected form is given by a modified form of the central limit theorem (Cramer 1946). Because the irradiance is modified by various physical processes, according to the central limit theorem, the observations will tend to be normally distributed and centered about a representative equivalent black-body temperature for either the cloud-top temperature or the earth's surface. The application of the central limit theorem is valid if there are no dominating physical effects from the violation of any assumption.

A more realistic channel 2 histogram of the cloud distribution represented by figure 1 is constructed in figure 2. Instead of two discrete lines, there are now two separate modes, indicating the cloudy and the clear subregions which are approximately normally distributed. The fractional coverage of each condition is given by the ratio of the area under each mode to the total area.

In the idealized model, it was assumed that the surface temperature was constant. In a more realistic model, the violation of this assumption tends to increase the variance of the mode representative of the irradiance received from the surface. This component of variance may be reduced by rescaling the abscissa from equivalent black-body temperature to a DV scale defined as the difference between the surface temperature and the observed equivalent

black-body temperature (Shenk 1963 and Panofsky et al. 1965). The new DV scale for the abscissa is presented in figure 2 for which surface temperature is assumed to be 303°K.

In regions where there are more than two cloud types with distinctly different top heights, more than two modes will be found in the actual distribution of channel 2 observations. In this situation, the definition for the fractional area covered by a single cloud type can be extended to the fractional area covered by the i th cloud type by

$$C_i = \frac{N_i}{N} \quad (1)$$

where C_i is the cloud coverage of i th type in percent, N_i is the number of observations under the i th mode, and N is the total number of observations in the region of interest.

Besides the cloud coverage information, the histograms also reveal information concerning cloud classification. Because clouds with the lowest equivalent black-body temperatures will have large vertical extent and high water content in a liquid or frozen state, the mode characterized by very high DV2s probably indicates a region of cumulonimbus activity or deep large-scale convection. The mode with the lowest DV2s will be observations from clear regions with high equivalent black-body temperatures. Intermediate sky conditions will be indicated by modes with typical values ranging between the extreme DV2's for the two examples. In some cases, however, no definite information about their types or heights can be derived directly from the histograms because cloud effective emissivities of the middle and upper troposphere vary with extremes from 0.16 to 1.0 (Kuhn 1963). Because of this variation, the upward irradiance value from a region with thick warm clouds of the middle troposphere may be identical to that from a region with thin, cold upper tropospheric clouds. Thus in an area which has both low-emissivity-valued clouds of the upper troposphere and thick high-emissivity-valued clouds of the middle troposphere, channel 2 histograms will not provide any discriminating information concerning either the types or the heights of their upper surface. However, the histograms will still provide total cloud coverage information.

For the situation in which the channel 2 histogram fails to discriminate between middle and upper tropospheric clouds, an alternative is to extend the single distribution model to a joint distribution model of channels 1 and 2, because channel 1 (the 6- μ m water vapor channel) is more sensitive to cloudiness and water vapor in the upper troposphere (Raschke 1966). Fritz and Rao (1967) have shown that the fractional transmission of the radiation through cirrus clouds is much larger for 10- μ m radiation (channel 2) than for 6- μ m radiation (channel 1). Histograms of channel 1 observations should reveal separate distinct modes associated with cirrus and middle-level cloudiness so that, even in situations where the first model fails, both cloud type and cloud-top heights could still

be inferred. The single distribution model for channel 1 observations is formed in the same manner as for the channel 2 model. Large DV1s indicate cirrus cloudiness while low-valued DV1s indicate a dry middle and upper troposphere. Because of strong absorption in the 6- μ m region, only a negligible portion of the upward irradiance in the water vapor region intercepted by the satellite is actually emitted from the earth's surface. Again, one expects that the actual distribution of channel 1 observations contains modes that, according to the central limit theorem, will tend to be approximately normally distributed because of the many factors influencing the 6- μ m irradiance.

In the actual construction of the two-dimensional arrays, the isopleths for local frequency maxima will delineate the modes of the specific sky conditions. From statistical considerations (i.e., the central limit theorem), these modes should be in the form of a bivariate joint normal distribution function. From physical considerations, the center with the lowest DV1 and DV2 values should indicate clear sky conditions, while the center with the highest DV1 and DV2 values indicate regions of cumulonimbus activity or deep large-scale convection. As for those centers with DV1 and DV2 values between the two extremes, the sky conditions they indicate may be quite complicated. However, according to the results of Fritz and Rao (1967), it is reasonable to assume that, in situations where two centers have approximately the same DV2 values but different DV1 values, the mode with higher DV1 should indicate cirrus clouds, while the mode with a lower DV1 should indicate lower clouds.

3. RESULTS

In the initial development of the technique to estimate cloud distributions from radiation data, a pilot study was conducted using only channel 2 data for four separate regions. These four areas are designated in table 1 and outlined in the HRIR (high resolution infrared) photo-strip shown in figure 3. Only the detailed results for the region B2 covering the area of the South Pacific from 105°W to 108°W and from 14°S to 23°S are presented to illustrate the preliminary tests. The MRIR channel 2 data were taken from Nimbus II orbit 213 of May 31, 1966. Sea-surface temperatures for the DV2 values were estimated from the May and June monthly mean temperatures for the South Pacific (U.S. Office of Naval Operations 1959).

The histogram of channel 2 radiation data is presented in figure 4. Two well-defined modes are found—one at DV2 equal to 7°K and the other at 15°K. For the region with DV2s greater than 20°K, the minor peaks that exist are not well defined.

For cloud coverage estimation, observations from the first three data intervals were assigned to the lowest class. They correspond to clear-sky conditions. Thus the percentage area is 30.5 percent for clear conditions and

TABLE 1.—Location, population, and model and visual estimates of cloud cover for blocks B1 to B4

Block no.	Latitudinal extent (°S)	Longitudinal extent (°W)	Total number of observations	Channel 2 model estimates (%)	Individual visual estimates (%)				Averaged visual estimates (%)
B1	1-12	102-105	300	5.0	25	20	20	20	21.2
B2	14-23	105-108	247	69.5	40	80	75	75	67.5
B3	26-34	109-113	210	82.4	75	90	85	65	78.7
B4	40-43	113-118	60	67.2	55	75	80	65	66.3

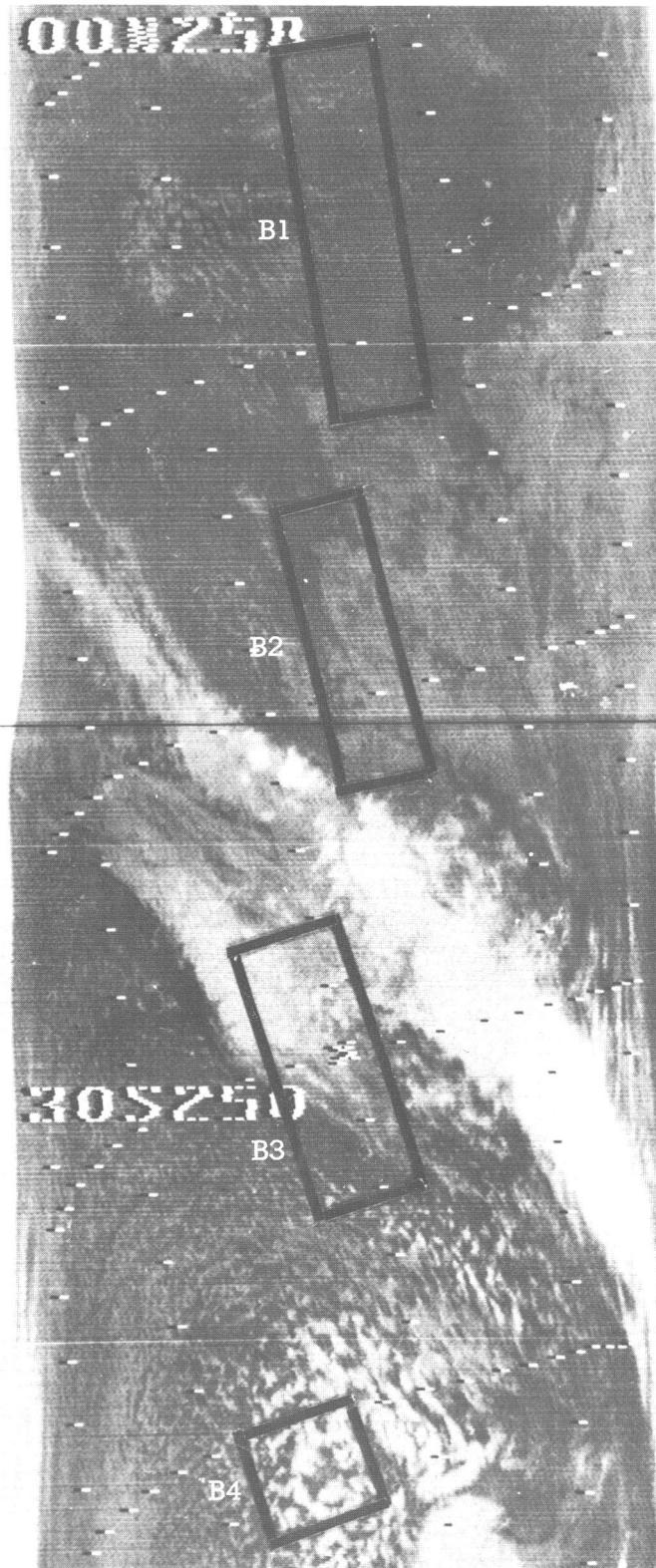


FIGURE 3.—HRIR photo strip for South Pacific, Nimbus II data from orbit 212 on May 31, 1966.

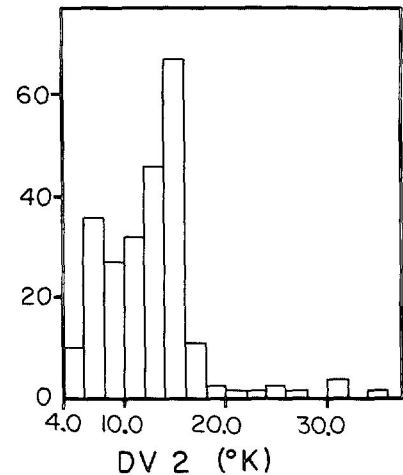


FIGURE 4.—Frequency histogram of DV2 data for block B2.

69.5 percent for cloudy conditions. In an independent check, four experienced meteorologists who were unaware of the MRIR estimates were asked to estimate the cloud coverage from the HRIR photo strip. It is interesting to note (table 1) that, while their estimates range from 40 to 80 percent, the mean estimate of 67.5 percent for region B2 agrees remarkably well with the estimate of 69.5 percent from the model.

The visual and model estimates of percentage cloud cover for the other three areas are summarized in table 1. The agreement between the cloud coverage estimates from the model and by the four meteorologists excellent for blocks 2, 3, and 4. The poor results for B1 are possibly due to a tendency for observers to overestimate cloud cover from satellite pictures for scattered conditions (Young 1967*a*, 1967*b*). In the histogram for B1 (not shown), the mode associated with the clear area dominates the mode associated with the low clouds. In addition, the two modes are not distinct because the temperature difference between the ocean surface and the top of the low scattered clouds is small. Note in the HRIR photo shown in figure 3 that the contrast between the clouds and ocean surface is slight in this region. In these situations where there is little contrast in the upward irradiance from the earth's surface and warm low clouds, this technique will fail.

The failure of this technique under the above condition is primarily due to the low resolution of the MRIR radiometer. The field of view at the subsatellite point of the MRIR radiometer on Nimbus II is a circle with a diameter of approximately 55.5 km. Due to the radiometer's low

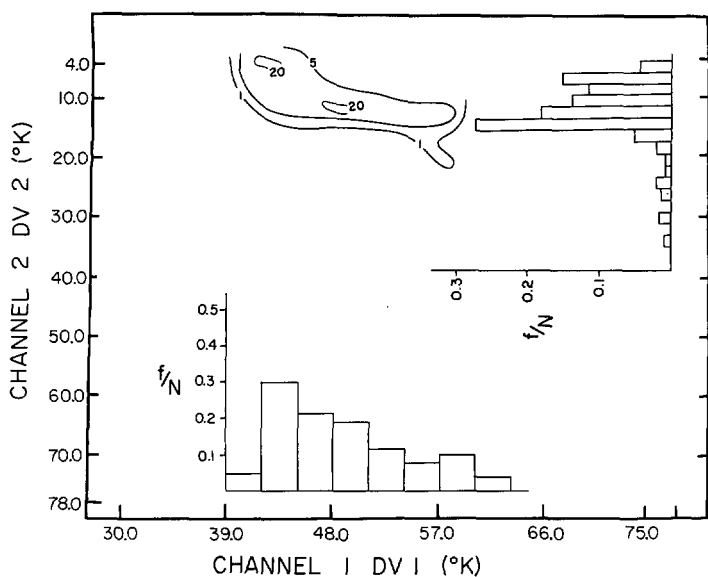


FIGURE 5.—Bivariate frequency and marginal probability density distributions of DV1 and DV2 data for region B2.

resolution, the observed value is the average of irradiances from clear and cloudy subregions in which the characteristic scale of small convective clouds is less than the field of view. If the technique were used with HRIR data, the modes associated with various cloud features should be more distinct because of the 8-km-diameter HRIR field of view. Further improvement in the technique would also be expected from an increased reliability of the modes due to a higher rate of sampling.

Although the preliminary study based on a univariate model revealed certain limitations in the direct inference of cloud distribution, the results indicated that large-scale cloud coverage can be inferred from the MRIR radiation data. In an attempt to improve the results, the bivariate model using both channel 1 and channel 2 data was applied to the same four regions. Figure 5 portrays the empirical joint distribution of DV1 and DV2 data for the region B2. The isopleths indicate the number of observations. Also indicated are the marginal probability densities for each channel. Two relative maxima are found. One is located at DV1 equal to 43°K and DV2 equal to 6°K; the other is located at DV1 equal to 48°K and at DV2 equal to 14°K. The upper left-hand maximum has the lowest possible DV1 and DV2 values of all centers from the scatter diagrams for the four regions. Thus it indicates not only a clear but also a dry atmosphere.

The mode in figure 5 located at DV values of 48°K and 14°K indicates the cloud coverage of 69.5 percent that was estimated in the preliminary study. Note that the DV2 marginal probability distribution along the right-hand edge of the figure portrays the two modes given in figure 4. In the DV1 marginal distribution, there are no distinct modes. However, when both distributions are considered simultaneously, the results indicate that the low value DV1s were primarily observed over the clear region while the DV1s greater than 49 were all observed over the cloudy region. In this study, no quantitative assessment

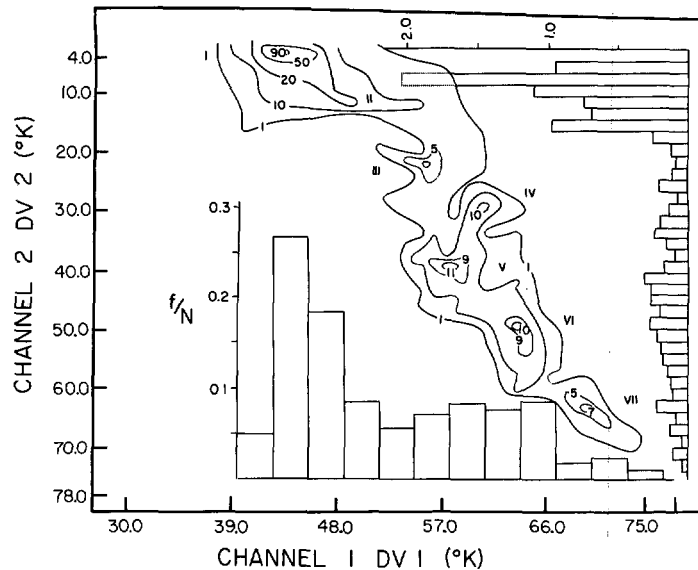


FIGURE 6.—Combined bivariate frequency and marginal probability density distributions of DV1 and DV2 data for regions B1 through B4.

of the amount of water vapor in the upper troposphere using Raschke's technique (1966) was made. Still, from Raschke and Bandeen's (1967) statement, "... that contributions (to a satellite observation) from irradiance in the 6.3 micron (now micrometer) region below 600 mb are small," it is possible to infer that the troposphere above the low-level clouds contained higher water vapor content than over clear areas. Furthermore, the negative skewness of the mode about the cloudy maxima in the bivariate distribution indicates a great variation of DV1 values above the clouds. In physical terms, the variance of water vapor content above the clouds was greater than in the clear drier subregion.

The DV2 histogram has a few higher valued observations which, along with the high-valued DV1 observations, indicate a trace of clouds higher in the troposphere. In the photo strip (fig. 3), the B2 area is partly clear and partly covered with warm low clouds; in the middle of the region, there is a trace of brighter clouds.

Figure 6 is a composite bivariate frequency distribution for all four regions. Seven relative maxima are identified by Roman numerals. One of the most interesting aspects of the combined figure is the definite organization of the field. Distinct maxima stand out in the two-dimensional portrayal while the local maxima of the medium- to high-valued portion of the marginal DV1 and DV2 distributions are much less pronounced. Thus, if one considers the distributions separately, one loses information concerning the cloud and water vapor structure of the atmosphere. For example, consider that the observations associated with modes III, IV, V, and VI were combined. Their marginal DV1 distribution would not be significantly different from the relatively uniform DV1 distribution in the interval from 51 to 66 indicated in figure 7. However, when the two-dimensional array is considered, it is clear that distinct cloud layers were present. Thus, it is important to form a cloud or irradiance model that preserves this im-

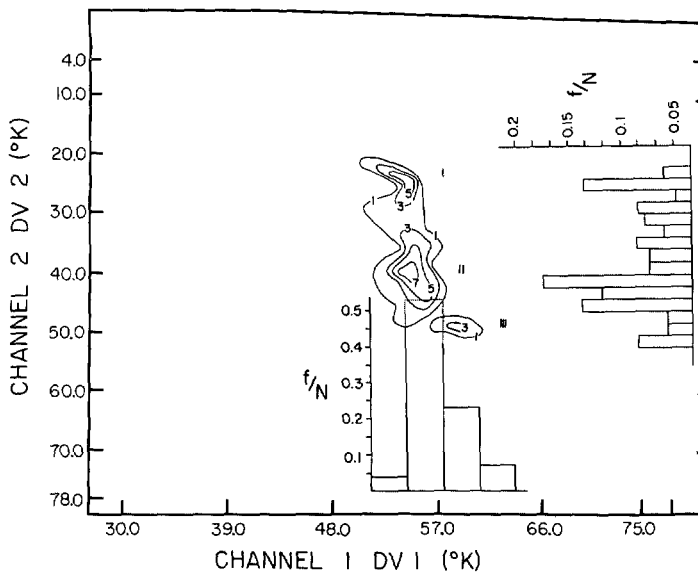


FIGURE 7.—Bivariate frequency and marginal probability density distribution of DV1 and DV2 data for region B4.

portant information in any extended general circulation climatology.

The most distinct maximum, I, is associated with the clear conditions. Note that local maxima are also present in both marginal distributions. Thus for this situation, one can conclude that clear regions are associated with lower values of middletropospheric and upper tropospheric water vapor content than cloudy areas.

The highest maximum, VII, is undoubtedly associated with the most intense convection in the cloudy regions. This mode is from region B3 data and is associated with the highest clouds in the extreme upper left-hand corner (fig. 3). Other relative maxima can be identified with cloud features in the various blocks and indicate that various cloud systems have identifiable irradiance fields that are distinct from each other.

The elongated region containing nearly all the observations of the bivariate frequency distribution of channels 1 and 2 portrays a general correlation between DV1 and DV2 that is primarily due to the presence or absence of clouds. However, for many purposes, it would be misleading to attempt to infer one from the other by correlation techniques. For example, the relative mode IV deviates from one linear relation connecting the extreme modes I and VII indicated in the diagram. Because the emissivity of cirrus clouds in the spectral region of channel 1 is greater than channel 2 (Fritz and Rao 1967), relative modes indicative of the cirrus clouds should be displaced to the right of the general linear relation.

The percentage area coverage of distinct cloud patterns associated with each mode is presented in table 2. The division of the distribution according to modes is not difficult except for the separation of modes I and II. Since most of the variance about strongly peaked mode I is likely associated with scattered low-level cloudiness, the

TABLE 2.—Percentage area coverage by the relative mode

Relative mode	Observational frequency	Percentage coverage
I	377	46.7
II	183	22.7
III	33	4.1
IV	25	3.1
V	99	12.3
VI	63	7.8
VII	27	3.3
Total	807	100.0

region of the distribution for DV1 greater than 46°K and DV2 greater than 10°K was combined with mode II. While it would be possible to speculate as to the type and height of cloud for all modes, there is no verifying information available. Hence, it seems advisable to attempt cloud identification in a later study when more complete data is available. The bivariate frequency distributions indicate that distinct modes are present that allow quantitative estimates of percentage cloud cover.

4. CONCLUSIONS AND SUGGESTIONS FOR FUTURE RESEARCH

The cloud cover estimation model developed and tested in this study provides a useful technique for quantitatively estimating cloud cover from satellite irradiance data. It will fail for situations in which the temperature difference between the earth's surface and the cloud-top surface is not significantly large. However, these situations are normally only associated with low clouds or for clouds over the extremely cold ice- and snow-covered polar regions. Over most regions in which there is considerable contrast in the upward irradiance from the earth's surface and the clouds, the technique using MRIR data shows considerable promise. With a higher resolution instrument, the relative modes in the bivariate distributions should be more pronounced with less variance, making the estimation more precise.

The use of monthly mean temperatures, instead of observed sea-surface temperatures in DV1 and DV2 calculations, may have caused errors in the locations of relative maxima and increased the variance of each mode in the histograms. Improvements can be expected when sea-surface temperature estimates from satellite information (Smith et al. 1970) are combined with the cloud inference techniques.

In future research for the development of a global cloud climatology, it is important to estimate cloud type and height. This should be possible with a higher resolution instrument since the variance of the relative modes would provide information on the uniformity of the irradiance from the upper cloud surface. Such information should identify whether the cloud is stratiform or cumuliform. Instruments designed with more appropriate spectral

regions are also desirable, for the accuracy of the detection of properties such as cirrus cloud amount and so on would be greatly improved. With the eventual identification of cloud type and height and the creation of a global cloud climatology, it may be possible to infer the vertical transport of important atmospheric properties by cloud convection.

ACKNOWLEDGMENT

The research was supported by the National Environmental Satellite Center, Environmental Science Services Administration, through ESSA Grant E-8-69(G).

REFERENCES

- Arking, Albert, "The Latitudinal Distribution of Cloud Cover From TIROS III Photographs," *Science*, Vol. 143, No. 3606, Feb. 7, 1964, pp. 569-572.
- Cramer, Harald, "Mathematical Methods of Statistics," *Princeton Mathematical Series*, Vol. 9, Princeton University, N.J., 1946, 575 pp. (see pp. 213-227).
- Davis, Paul A., "An Analysis of the Atmospheric Heat Budget," *Journal of Atmospheric Sciences*, Vol. 20, No. 1, Jan. 1963, pp. 5-22.
- Fritz, Sigmund, and Rao, P. Krishna, "On the Infrared Transmission Through Cirrus Clouds and the Estimation of Relative Humidity From Satellites," *Journal of Applied Meteorology*, Vol. 6, No. 6, Dec. 1967, pp. 1088-1096.
- Houghton, Henry G., "On the Annual Heat Balance of the Northern Hemisphere," *Journal of Meteorology*, Vol. 11, No. 1, Feb. 1954, pp. 1-9.
- Katayama, Akira, "On the Radiation Budget of the Troposphere Over the Northern Hemisphere, Pt. 1," *Journal of the Meteorological Society of Japan*, Ser. 2, Vol. 44, No. 6, Tokyo, Dec. 1966, pp. 381-401.
- Kuhn, Peter M., "Measured Effective Long-Wave Emissivity of Clouds," *Monthly Weather Review*, Vol. 91, No. 10-12, Oct.-Dec. 1963, pp. 635-640.
- London, Julius, "Study of the Atmospheric Heat Balance," *Progress Report No. 131.06, Contract No. AF19(122)-165, College of Engineering, New York University, N.Y., May 1951, 21 pp.*
- Manabe, Syukuro, and Möller, Fritz, "On the Radiative Equilibrium and Heat Balance of the Atmosphere," *Monthly Weather Review*, Vol. 89, No. 12, Dec. 1961, pp. 503-532.
- Panofsky, Hans A., Schwalb, Arthur, Lethbridge, Mae D., Huang, Chin-Hua, Frash, Clifford, and Bradford, Robert, "Synoptic Applications of Infrared Satellite Data," *Interim Report, 1 January 1965-31 October 1965*, Grant No. WBG-48, Department of Meteorology, Pennsylvania State University, University Park, Oct. 31, 1965, 32 pp.
- Raschke, Ehrdard, "Tropospheric Water Vapor Content and Surface Temperature From TIROS IV Radiation Data," *NASA Contract Report No. 595, National Aeronautics and Space Administration, Washington, D.C., Sept. 1966, 110 pp.*
- Raschke, Ehrdard, and Bandeen, William R., "A Quasi-Global Analysis of Tropospheric Water Vapor Content From TIROS IV Radiation Data," *Journal of Applied Meteorology*, Vol. 6, No. 3, June 1967, pp. 468-481.
- Rasool, S. I., "Cloud Heights and Nighttime Cloud Cover From TIROS Radiation Data," *Journal of the Atmospheric Sciences*, Vol. 21, No. 2, Mar. 1964, pp. 152-156.
- Shenk, William E., "TIROS II Window Radiation and Large Scale Vertical Motion," *Journal of Applied Meteorology*, Vol. 2, No. 6, Dec. 1963, pp. 770-775.
- Smith, William L., Rao, P. Krishna, Koffler, Russell, and Curtis, W. R., "The Determination of Sea-Surface Temperature From Satellite High Resolution Infrared Window Radiation Measurements," *Monthly Weather Review*, Vol. 98, No. 8, Aug. 1970, pp. 604-611.
- U.S. Office of Naval Operations, *U.S. Navy Marine Climatic Atlas of the World, Vol. 5, South Pacific Ocean, NAVAER 50-1C-532, Nov. 1, 1959, 15 pp. plus 267 charts.*
- Winston, Jay S., and Taylor, V. Ray, "Atlas of World Maps of Long-Wave Radiation and Albedo," *ESSA Technical Report NESC-43, National Environmental Satellite Center, Suitland, Md., Sept. 1967, 32 pp.*
- Young, Murray J., "Variability in Estimating Total Cloud Cover From Satellite Pictures," *Journal of Applied Meteorology*, Vol. 6, No. 3, June 1967a, pp. 573-579.
- Young, Murray J., "Reply to Comments on 'Variability in Estimating Total Cloud Cover From Satellite Pictures,'" *Journal of Applied Meteorology*, Vol. 6, No. 6, Dec. 1967b, p. 1128.

[Received July 13, 1970; revised March 5, 1971]